Discrete-Time Memristor Model for Enhancing Chaotic Complexity and Application in Secure Communication

Wenhao Yan (ywh0512@163.com)
Heilongjiang University https://orcid.org/0000-0001-9237-7996
Zijing Jiang
Heidelberg University
Qun Ding
Heilongjiang University https://orcid.org/0000-0002-5520-6001

Research Article

Keywords: TiO2 memristor model, Discrete time memristor, Fixed point, Secure communication.

Posted Date: January 5th, 2022

DOI: https://doi.org/10.21203/rs.3.rs-1214130/v1

Noname manuscript No.
(will be inserted by the editor)

Discrete-time Memristor Model for Enhancing Chaotic Complexity and Application in Secure Communication

Wenhao Yan · Zijing Jiang · Qun Ding

Received: date / Accepted: date

Abstract The physical implementation of continuous-time memristor makes it widely used in chaotic circuits, whereas discrete-time memristor has not received much attention. In this paper, the backward-Euler method is used to discretize TiO2 memristor model, and the discretized model also meets the three fingerprinter characteristics of the generalized memristor. The short period phenomenon and uneven output distribution of one-dimensional chaotic systems affect their applications in some fields, so it is necessary to improve the dynamic characteristics of one-dimensional chaotic systems. In this paper, a two-dimensional discrete-time memristor model is obtained by linear coupling the proposed TiO2 memristor model and one-dimensional chaotic systems. Since the two-dimensional model has infinite fixed points, the stability of these fixed points depends on the coupling parameters and the initial state of the discrete TiO2 memristor model. Furthermore, the dynamic characteristics of one-dimensional chaotic systems can be enhanced by the proposed method. Finally, we apply the generated chaotic sequence to secure communication.

Keywords TiO2 memristor model · Discrete time memristor · Fixed point · Secure communication

1 Introduction

In 1971, Professor Chua, a Chinese-American scientist, theoretically predicted the existence of a nonlinear passive electronic component between charge and magnetic flux according to the theory of electronics, named it as the memristor and proposed the concept of generalized memristor[1,2]. For a long time, due to the lack of suitable materials, the research of memristor has been in the theoretical stage. Until 2008, HP Laboratory in the United States manufactured solid memristor by using double-layer TiO2 thin film, which made the memristor model physically realized[3]. In 2013, Adhikari and Biolek[4,5] proposed three fingerprints of memristor, that is, adding bipolar periodic signals, the device is a tight hysteresis loop passing through the origin on the plane, and its response is periodic. When the frequency exceeds the critical value, the area of hysteresis sidelobe decreases monotonically with the increase of frequency. As the frequency increases to infinity, the tight hysteresis loop of the device degenerates into a single-valued function. As the memristor is a nonlinear component and has memory capability, memristor is widely used in neural network[6–8], nonlinear circuit system[9,10], nanotechnology[11], electrical engineering[12,13]and other fields.

Chaos is an inherent randomness of deterministic systems and a special motion of nonlinear dynamic systems widely existing in nature[14]. Due to the defects of the low-dimensional discrete chaotic system, such as simple algebraic structure and few control parameters, the system output has a short period and the value distribution of the sequence is not uniform[15, 16]. So a lot of work is done to enhance the dynamics of low-dimensional discrete chaotic systems. Zhou et al.[17] proposed a parametric switching chaotic system and applied it to image encryption schemes. Hua et al.[18,19]took the output of low-dimensional system as the input of nonlinear function to improve the dynamic characteristics of low-dimensional chaotic sys-

W. Yan · Z. Jiang · Q. Ding(✉)
Electronic Engineering College, Heilongjiang University, Harbin 150080, China
E-mail: qunding@aliyun.com

W. Yan
E-mail: ; 1202873@s.hlju.edu.cn

tem. All these works were based on mathematical concepts without physical background. In 2008, Professor Chua[20] replaced the original Chua diode with a memristor in a chaotic circuit, and the results show that the circuit can also generate chaotic behavior. Later, scholars have done a lot of research on the memristor chaotic system, such as multi-stable states [21,22], coexistence attractor [23,24], hidden attractor[25]. However, all these work are based on continuous-time memristor models(CMM). Compared with CMM, discrete-time memristor models (DMM) have not received much attention. In recent years, Peng et al.[26] proposed a discrete-time ideal charge-controlled memristor model. The output of the model was used as a control parameter of the two-dimensional Hénon mapping, and the output of the Hénon mapping was disturbed to enhance the dynamic characteristics of the Hénon mapping. Bao et al. [27] proposed a discrete discrete time ideal charge-controlled memristor model, and linearly coupled the model with Logistic map to obtain a new two-dimensional memristor model. Deng et al. [28] also proposed a two-dimensional hyperchaotic system based on discrete memristor and analyzed the nonparameteric bifurcation mechanism of the system. However, the above work is only based on a single low-dimensional discrete chaotic system. In this paper, a generalized two-dimensional hyperchaotic system based on discrete memristor is proposed. The discrete memristor is coupled with classical Logistic map, Sine map and Tent map respectively to generate two-dimensional memristor chaotic map. These three models are chaotic in a wide range of parameters, and even hyperchaotic in a suitable range of parameters. This method is simple and effective to enhance the dynamic characteristics of chaotic systems.

The rest of this paper is arranged as follows: In Section 2, the TiO2 memristor model is discretized by using the backward-Euler method, and the discretized model also conforms to the essential characteristics of the generalized memristor. Then, the TiO2 memristor model is linearly coupled with the one-dimensional chaotic system to obtain the two-dimensional discrete memristor map. In Section 3, three numerical examples are given and the three systems are evaluated by chaotic dynamics characteristic index and complexity analysis. In Section 4, three systems are used as chaotic sequence generators of chaotic keying communication scheme, and the advantages and disadvantages of chaotic sequence are evaluated by the bit error rate of communication scheme. Finally, some conclusions are draw in Section 5.

Table 1 Mathematical models of three continuous-time memristors

CMs	charge-controlled	flux-controlled
ideal	$\begin{cases} v(t)=M(q)i(t) \\ dq/dt=i(t) \end{cases}$	$\begin{cases} i(t)=W(\phi)v(t) \\ d\phi/dt=v(t) \end{cases}$
general	$\begin{cases} v(t)=M(x)i(t) \\ dx/dt=f(x,i) \end{cases}$	$\begin{cases} i(t)=W(x)v(t) \\ dx/dt=v(x,v) \end{cases}$
generalized	$\begin{cases} v(t)=M(x,i)i(t) \\ dx/dt=i(x,i) \end{cases}$	$\begin{cases} i(t)=W(x,v)v(t) \\ dx/dt=v(x,v) \end{cases}$

2 Two dimensional generalized discrete memristor coupling model

In 2014, Professor Chua [29] proposed three mathematical expressions of time-varying memristor(i.e., CMM), namely three different memristor models. At the same time, according to the input signal of the memristor, each model is divided into charge-controlled memristor and flux-controlled memristor. The mathematics expression of these are shown in Table 1, where $M(\cdot)$ is the memristance function based on the charge-controlled memristor, while $W(\cdot)$ is the memristance function based on the magnetic flux-controlled memristor. In the ideal model, $M(\cdot)$ is only a function of charge q, and the derivative of charge q is the current i through the device, while $W(\cdot)$ is only a function of magnetic flux ϕ, The derivative of magnetic flux ϕ is the voltage v at both ends of the device. In the general model, $M(\cdot)$ is only a function of the system state variable x, and the derivative of the system variable x is a function of the state variable x and the current i flowing through the device, denoted by $f(x,i)$, while $W(\cdot)$ is also a function of the system state variable x, and the derivative of the system variable x is a function of the state variable x and the voltage v both ends of the device, denoted by $g(x,v)$. In the generalized model, $M(\cdot)$ is the function of the system state variable x and the current i flowing through the device, and the derivative of the system variable x is a function of the state variable x and the current i flowing through the device, denoted by $f(x,i)$, while $W(\cdot)$ is the function of the system state variable x and the voltage v at both ends of the device, and the derivative of the system variable x is a function of the state variable x and the voltage v both ends of the device, denoted by $g(x,v)$. In this paper, we take the ideal charge-controlled memristor model as the research object, so we can get a charge-controlled memristor characterized by voltage $v(t)$ and current $i(t)$, and the mathematics expression is as follows

$$\begin{cases} v(t)=M(q)i(t) \\ dq(t)/dt=i(t) \end{cases} \tag{1}$$

where $v(t)$ and $i(t)$ is the voltage and the input current of the memristor, and $q(t)$ is the charge the memristor at time t. The relationship between charge $q(t)$ and input current $i(t)$ is written as

$$q(t) = q(t_0) + \int_{-\infty}^{t} i(t)dt, \tag{2}$$

where $q(t_0)$ is the initial charge of memristor. After discretization by the backward- Euler method, and the mathematical expression of the discretized model is as follows:

$$\begin{cases} v_n = M(q_n)i_n \\ q_{n+1} = q_0 + h\sum_{j=1}^{n} i_j \end{cases} \tag{3}$$

where, h represents the step size required for each iteration. Generally, suppose $h = 1$. In this paper, the memristance function $M(q_n)$ is based on TiO2 memristor model, and the mathematical expression of $M(q_n)$ for the function can be obtained as

$$M(q_n) = (R_1 q_n + R_2 {q_n}^2), \tag{4}$$

where $R_1 = R_{OFF}$, $R_2 = R_{OFF}\mu_V R_{ON}/D^2$. However, R_{OFF} is the undoped partial voltage, R_{ON} is the doped partial voltage, μ_V is the length of the memristor element, and D is the average ion mobility. In this paper, set $R_1 = -2, R_2 = 1$. In order to illustrate the characteristics of the discrete-time TiO2 memristor model, a discrete sine current signal $i_n = A\sin(\omega t)$ is added to the memristor. The amplitude curves of current i_n and voltage v_n of the memristor are shown in Fig.1. Given A, ω, and q_0 in detials, the iterative sequences of current i_n and voltage v_n are shown in Fig. 1(a). By fixing A, q_0, the pinched hysteresis loop of the memeristor at different frequencies ω are simulated in Fig. 1(b). It can be seen that the area of pinched hysteresis loop decreases with the increase of frequencies ω. By fixing ω, q_0, the pinched hysteresis loop of the memeristor at different amplitude A are plotted in Fig. 1(c). In addition, by fixing A, ω, the pinched hysteresis loop of the memeristor at initial charge q. are depited in Fig. 1(d). The above simulation results show that the discrete memristor model meets the characteristics of generalized memristor.

2.1 Memristor coupled low-dimensional discrete chaos model

Due to its simple algebraic structure, one-dimensional discrete chaotic systems such as Logistic map, Sine map and Tent map have defects such as short period phenomenon, uneven distribution of output sequence and predictable motion trajectory. However, these defects will limit the application of one-dimensional chaotic systems in some security fields. In order to enhance the chaotic dynamics characteristics of one-dimensional chaotic maps, a generalized two-dimensional discrete memristor model (2D-DMM) is obtained by coupling one-dimensional chaotic systems with the discrete memristor model constructed above. The structural block diagram of 2D-DMM is shown in Fig. 2, where $F(\mu, x_n)$ is the one-dimensional chaotic model, μ is the control parameter of it, and the parameter k is the coupling coefficient between the chaotic map and the discrete memristor model. The mathematical expression of 2D-DMM can be obtained

$$\begin{cases} x_{n+1} = F(\mu, x_n) + k(R_1 q_n + R_2 {q_n}^2)x_n \\ q_{n+1} = x_n + q_n \end{cases} \tag{5}$$

According to Eq. 5, based on different one-dimensional discrete chaotic systems, corresponding two-dimensional discrete memristor models can be obtained by using this system framework. This model combines the outputs of two nonlinear systems linearly to improve the dynamics of one system. This method is simple and effective to enhance the dynamic characteristics of chaotic systems.

The stability of discrete chaotic system is described by its fixed point, which means that the value of iteration at the next moment is the same as the value at this moment. The fixed point of Eq. 5 is denoted as$(\tilde{x}, \tilde{q})$, and one can obtain the following expression.

$$\begin{cases} \tilde{x}_n = F(\mu, \tilde{x}_n) + k(R_1\tilde{q}_n + R_2\tilde{q}_n^2)\tilde{x}_n \\ \tilde{q}_n = \tilde{x}_n + \tilde{q}_n \end{cases} \tag{6}$$

Obviously, when $F(\mu, x) = 0$, the system has infinite fixed points, which are expressed as

$$S = (\tilde{x}, \tilde{q}) = (0, \xi) \tag{7}$$

where ξ is an arbitrary real number. While $F(\mu, x) \neq 0$, since Eq.6 has no real root, the system has no fixed point. The Jacobin matrix of Eq. 5 is shown as follows

$$J = \begin{bmatrix} k(R_1 q_n + R_2 {q_n}^2) + \phi(\mu) & k(R_1 q_n + R_2 {q_n}^2)x_n \\ 1 & 1 \end{bmatrix}, \tag{8}$$

where $\phi(\mu) = dF(\mu, x_n)/dx_n$. The eigenvalue polynomial at the fixed point S of Eq. 5 can be obtained

$$P(\lambda) = (\lambda - 1)(\lambda - k(R_1 q_n + R_2 {q_n}^2) - \phi(\mu)). \tag{9}$$

Therefore, the two eigenvalues at fixed points S of Eq.5 are calculated as

$$\lambda_1 = 1, \lambda_2 = k(R_1 q_n + R_2 {q_n}^2) - \phi(\mu). \tag{10}$$

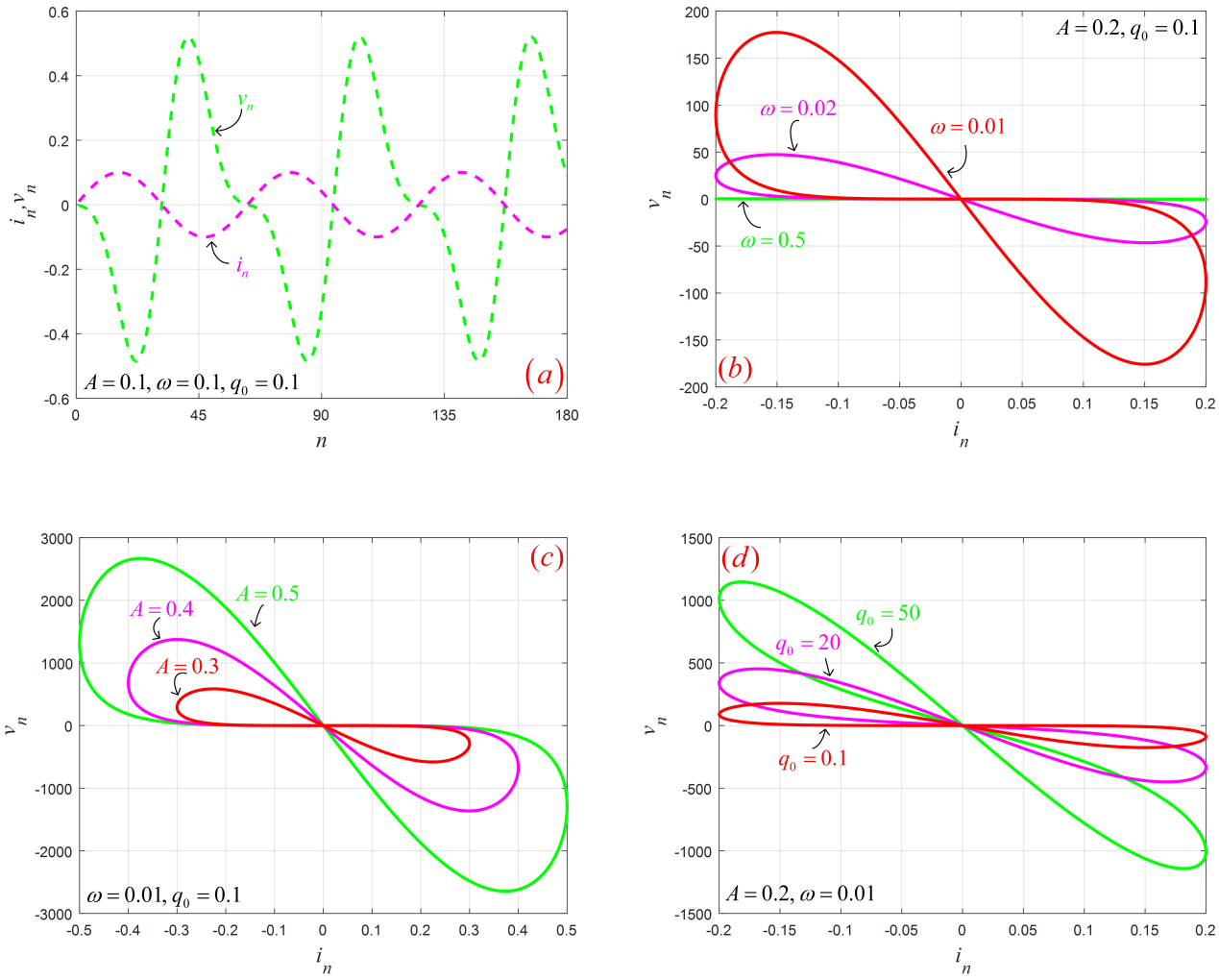

Fig. 1 The $i_n - v_n$ amplitude curves of the memeristor: **a** i_n and v_n iterative sequences; **b** The pinched hysteresis loop of the memeristor at different frequencies ω; **c** The pinched hysteresis loop of the memeristor at different amplitude A; **d** The pinched hysteresis loop of the memeristor at different initial charge q.

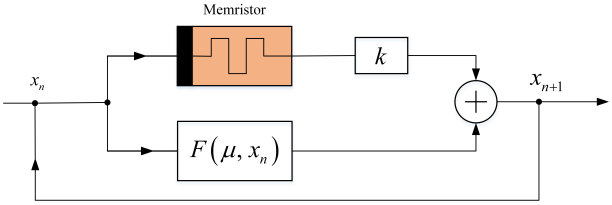

Fig. 2 Structure block diagram of two-dimensional discrete memristor model

According to the stability criterion of fixed points, When the modules of the two eigenvalues are in the unit circle, the fixed point is stable, otherwise it is unstable. Since λ_1 is always on the unit circle, whether λ_2 is inside or outside the unit circle depends on $\phi(\mu)$, the coupling coefficient k, and the initial state ξ of the memristor. Therefore, the fixed points S of the model may be stable or unstable. While $F(\mu, x) \neq 0$, the Eq.6 has no fixed point. In this case, the trajectory of the map is periodic, chaotic, or even hyperchaotic.

3 Numerical example of two-dimensional discrete memristor model

In this Section, we construct the corresponding two-dimensional discrete memristor model based on Logistic map, Sine map and Tent map, respectively. In addition, the performance of their chaotic sequences will be evaluate.

3.1 Numerical examples

According to Eq. 5, 2D-DMM based on Logistic map, Sine map and Tent map can be obtained, respectively. The mathematical expression of the two-dimensional discrete memristor coupled-Logistic model (2D-DMLM) is as follows

$$\begin{cases} x_{n+1} = \mu x_n(1-x_n) + k(R_1 q_n + R_2 {q_n}^2)x_n \\ q_{n+1} = x_n + q_n \end{cases} \tag{11}$$

where μ is the control parameter of Logistic map, $F(\mu, x) = 0$, and $\phi(\mu) = \mu$. The mathematical expression of the two-dimensional discrete memristor coupled-Sine model (2D-DMSM) is described as

$$\begin{cases} x_{n+1} = \mu \sin(2\pi x_n) + k(R_1 q_n + R_2 {q_n}^2)x_n \\ q_{n+1} = x_n + q_n \end{cases} \tag{12}$$

where μ is the control parameter of Sine map, $F(\mu, x) = 0$, and $\phi(\mu) = 2\pi\mu$. The mathematical expression of the two-dimensional discrete memristor coupled-Tine model (2D-DMTM) is obtained as

$$\begin{cases} x_{n+1} = \begin{cases} \mu x_n + k(R_1 q_n + R_2 {q_n}^2)x_n, x_n < 0.5 \\ \mu(1-x_n) + k(R_1 q_n + R_2 {q_n}^2)x_n, x_n \geq 0.5 \end{cases} \\ q_{n+1} = x_n + q_n \end{cases} \tag{13}$$

where μ is the control parameter of Tent map, $F(\mu, x) = 0$, and $\phi(\mu) = \pm\mu$. The mathematical expressions of the three models are given in this section, and the chaotic performance evaluation of the three models is given in the following section.

3.2 Bifurcation with coupling strength

The bifurcation diagram of chaotic system is an important tool to analyze its characteristics. It can directly observe the period-doubling bifurcation and chaotic state of the system under different control parameters. Lyapunov exponent(LE) is an important index to measure the separation rate of adjacent trajectorys in phase space. In this paper, Wolf's Jacobin algorithm is used to calculate LE. The LE can be calculated as follows

$$LE = \lim_{n \to +\infty} \frac{1}{n} \sum_{i=0}^{n-1} \ln(\lambda_i), \tag{14}$$

where i represents the number of iterations of the system, while λ_i is the eigenvalue of the Jacobin matrix of the system after i iterations. For a chaotic system. At least it should have a positive LE. The larger the value of LE is, the stronger the chaotic characteristics of the system will be. When the number of positive LE is greater than 1, the system is a hyperchaotic system, indicating that the system has stronger chaotic characteristics. Given control parameter μ and initial conditions (x_0, q_0), the bifurcation diagram and LE spectrum of the change of coupling coefficient k of the models are shown in Fig. 3. As can be seen from Fig. 3, under different coupling coefficients, the three models exhibit complex dynamic properties, such as periodic Windows, periodic or period-like states, chaos and hyperchaotic states. It is worth noting that 2D-DMLM and 2D-DMTM enter chaos state from period-doubling way, while 2D-DMSM enters chaos state from periodic state in period-like way. Given controlle parameter μ, initial conditions (x_0, q_0), and coupling coefficient k, the two Lyapunov exponents for the three models are given in Table 2. Note that the length of the sequence is set to 10^5. It can be seen that the three models all have two positive LEs, indicating that the three models are all hyperchaotic.

Table 2 The two Lyapunov exponents of three models

Iterms	μ	k	(x_0, q_0)	LE_1, LE_2
2D-DMLM	0.200	1.99	(0.3,0.7)	0.3028, 0.0731
2D-DMSM	-0.05	1.82	(0.2,0.4)	0.3200, 0.0757
2D-DMTM	-0.40	1.58	(0.1,0.6)	0.2797, 0.1062

3.3 Hyperchaotic attractor

From subsection 3.2, we know that the three models are in hyperchaotic state with determined parameters. This section will study the hyperchaotic sequences generated by three models. Given control parameter μ, initial conditions (x_0, q_0), and coupling coefficient k in detials respectively, the trajectories of the three models in phase space are shown in Fig. 4. It can be seen that all hyperchaotic attractors are distributed in a bounded region and have complex fractal structures. Secondly, hyperchaotic sequences generated by the three models are shown in Fig. 5. The three sequences are all similar to noise signals, and the magnitude of sequence values is irregular and aperiodic. Next, we will evaluate the performance of hyperchaotic sequences through Sample entropy(SE)[30], Permutation entropy(PE)[31], Correlation dimension(CorDim)[32], Kaplan-Yorke dimension(KYDim)[33]. Note that the length of the sequence is set to 10^5. The calculation results of the three hyperchaotic sequences are shown in Table 3. It can be seen that the hyperchaotic sequence generated by the system has excellent complexity and can be used in image encryption, chaotic secure communication and other fields. Secondly, the discrete memristor model based

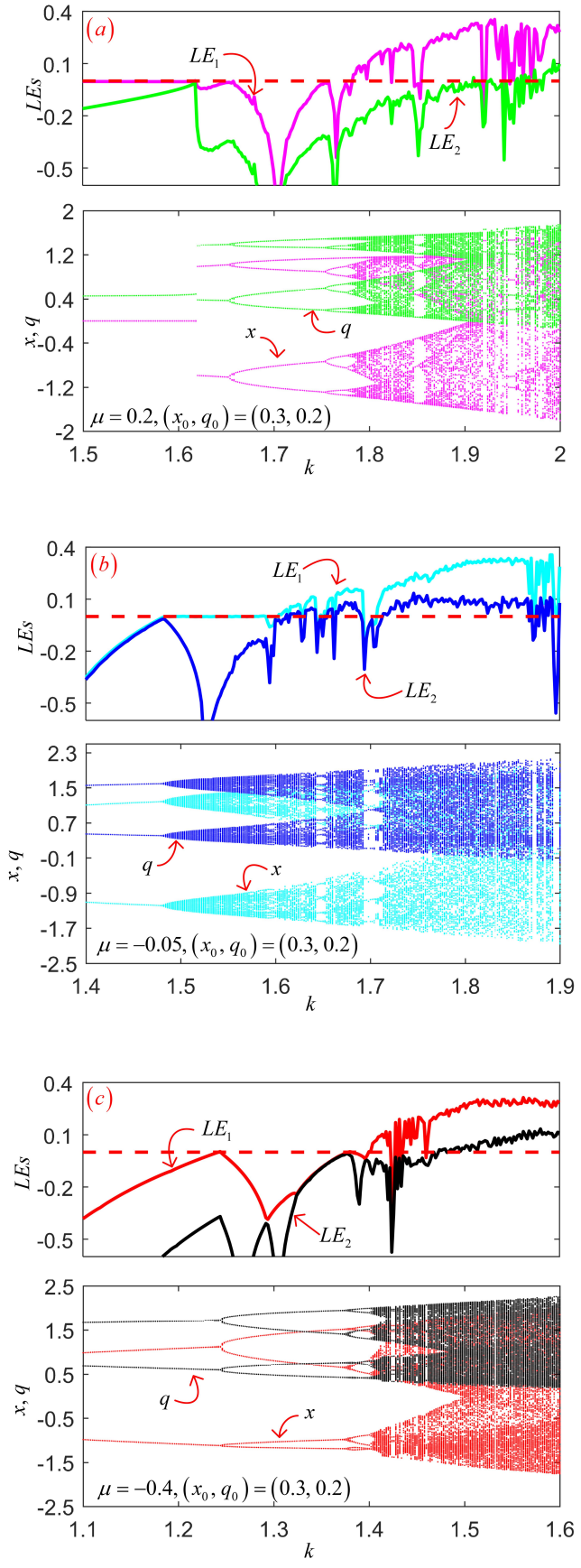

Fig. 3 The bifurcation and LEs of three models: textbfa32D-DMLM, **b** 2D-DMSM; **c** 2D-DMTM.

Table 3 Performance of hyperchaotic sequences generated by three models

Iterms	SE	PE	CorDim	K-YDim
2D-DMLM	0.7268	0.8311	1.6163	2
2D-DMSM	0.7786	0.8010	1.6315	2
2D-DMTM	0.7076	0.8216	1.6295	2

on chaotic system can enhance the complexity of one-dimensional chaotic system.

4 Application of hyperchaotic sequence in secure communication

Due to the unpredictability and ergodicity of chaotic systems, chaotic systems are widely used to transmit data safely through various networks. When chaotic system is used for data transmission, the distribution of its output has great influence on the performance of transmission error resistance. In this section, we take the three chaotic sequences as the chaotic sequence generators of the chaotic keying communication model and evaluate the sequences by the bit error rate of signal in the process of transmission with noise. In this paper, chaotic keying communication model is used as the reference modulation-differential chaotic shift keying model(RM-DCSK). The RM-DCSK scheme consists of a transmitter and a receiver. The transmitter first uses chaotic sequence to encode the information bits to generate the transmission signal, and then sends the transmission signal to the receiver. The receiver decodes the received signal to recover bits of information.

4.1 Transmitter Sructure

The transmission signal structure in RM-DCSK is depited in Fig. 6, where a frame singal is made up with two neighboring slots. Take the k frame signal for example, the chaotic sequence x_k is sent on the basis of information bit $b_{2k} \in \{-1, +1\}$ in first slot. However, the signal of the second time slot is the sum of two parts,he first part is the modulation of information bit $b_{2k+1} \in \{-1, +1\}$ and the transmission signal of the first time slot; the second part is the chaotic sequence of this slot. Set the length of chaotic sequence to M, and the mathematical expression of the k-frame signal s_i is as follows

$$s_i = \begin{cases} b_{2k} x_i, 2kM < i \leq (2k+1)M \\ b_{2k+1} b_{2k} x_{i-M} + x_i, (2k+1)M < i \leq 2(k+1)M \end{cases} \tag{15}$$

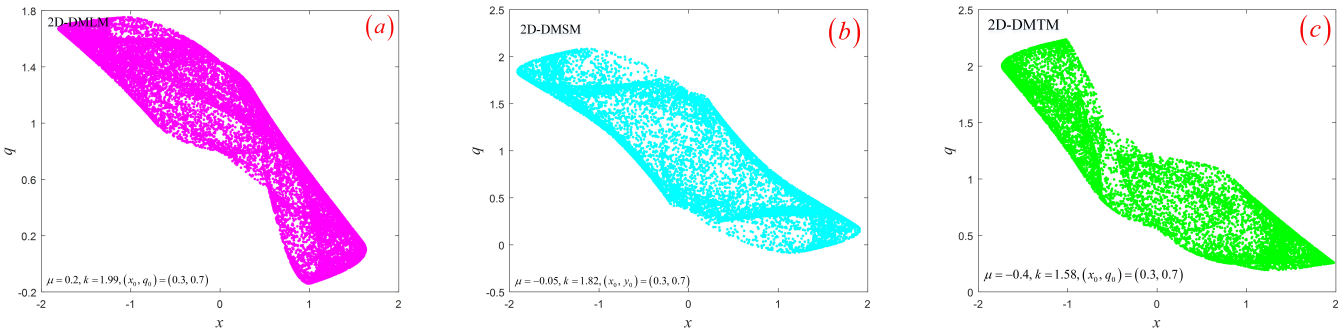

Fig. 4 The phase space trajectory of three models: textbfa32D-DMLM, **b** 2D-DMSM; **c** 2D-DMTM.

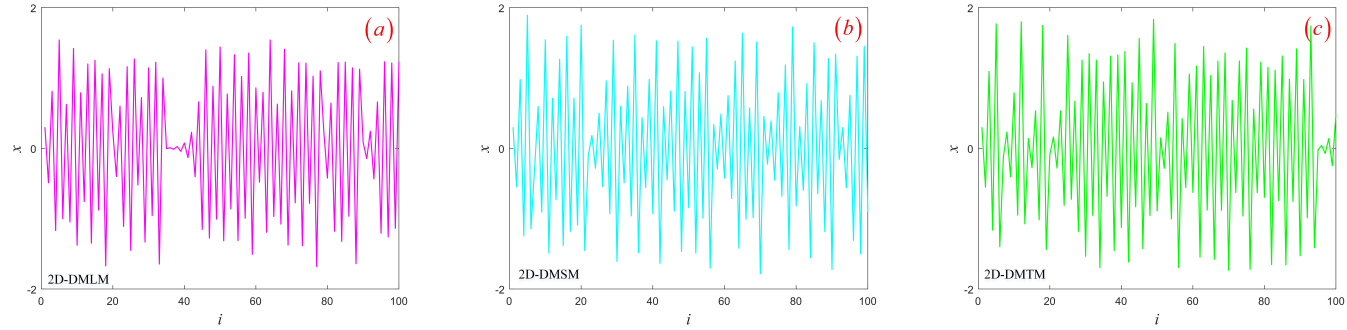

Fig. 5 The hyperchaotic sequence produced by three models: **a3**2D-DMLM, **b** 2D-DMSM; **c** 2D-DMTM.

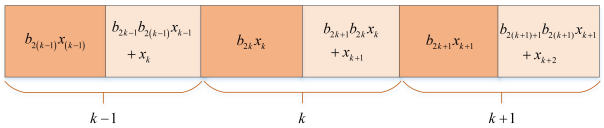

Fig. 6 Structure of transmission signal in RM-DCSK

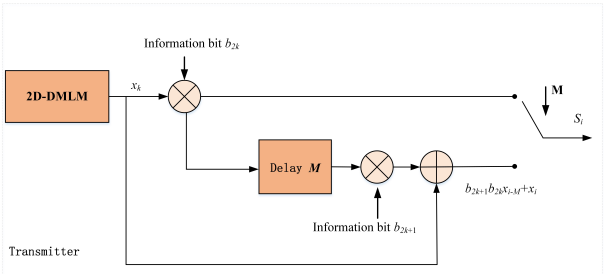

Fig. 7 Structure of transmission signal in RM-DCSK

where x_i satisfies the following conditions

$$x_{(2k+1)M+m} = x_{2(k+1)M+m}, 0 < m \leq M; k \in \mathbb{Z}. \quad (16)$$

4.2 Receive Sructure

When the receiver receives a transmission signal from the sender, the correlator can be used to recover the original bits of information. The RM-DCSK system mainly utilizes chaotic delay characteristics and noncoherent demodulation. The structure diagram of the receiving end is shown in Fig. 8. Since signals may be interfered by noises when transmitted in different networks, the received signals are different from the original signals. In this paper, the Additive White Gaussian Noise (AWGN) channel model is used as the main communication transmission medium. The interference in the channel is mainly the noise signal ζ, so the received signal r_i is as follows:

$$r_i = s_i + \zeta_i. \quad (17)$$

The output of the correlator Z_n is the product of the received signal r_i and its delayed version r_{i-M}. Therefore, the mathematical expression of correlator Z_n is calculated as the sum

$$Z_n = \sum_{i=nM+1}^{(n+1)M} r_i r_{i-M}. \quad (18)$$

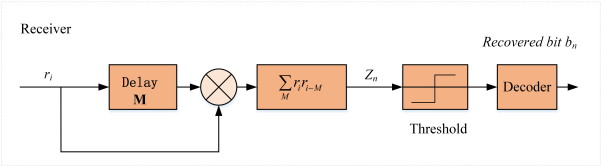

Fig. 8 Structure of transmission signal in RM-DCSK

Then, the mathematical expression of correlator Z_{2k} for recovering bit b_{2k} is rewritten as the sum

$$\begin{aligned} Z_{2k} &= \sum_{i=2kM+1}^{(2k+1)M} (s_i + \zeta_i)(s_{i-M} + \zeta_{x_{i-M}}) \\ &= \sum_{i=2kM+1}^{(2k+1)M} (b_{2k-1}b_{2(k-1)}x_{i-2M} + x_{i-M} + \zeta_{i-M}) \\ &\times (b_{2b}x_i + \zeta_i). \end{aligned} \tag{19}$$

Eq.23 tells us that $x_{i-M} = x_i$, then Eq.19 can be simplified as

$$\begin{aligned} Z_{2k} &= \sum_{i=2kM+1}^{(2k+1)M} (b_{2k-1}b_{2(k-1)}x_{i-2M} + x_{i-M} + \zeta_{i-M}) \\ &\times (b_{2b}x_i + \zeta_i) \\ &= b_{2k} \sum_{i=2kM+1}^{(2k+1)M} {x_i}^2 + \sum_{i=2kM+1}^{(2k+1)M} x_i A_i \end{aligned} \tag{20}$$

where A_i is calculated as follows:

$$\begin{aligned} Z_{2k} &= b_{2k}b_{2k-1}b_{2(k-1)}x_i x_{i-2M} + b_{2k}x_i\zeta_{i-M} \\ &+ b_{2b-1}b_{2(b-1)}x_{i-2M}\zeta_i + x_i\zeta_i + \zeta_i\zeta_{i-M}. \end{aligned} \tag{21}$$

Since the noise signal is much less energy than the useful signal, so the square term containing chaotic signal is the signal of subject discrimination. Then the positive and negative of the correlator Z_{2k} is mainly determined by the bit information b_{2k}. In addition, the correlator Z_{2k+1} can similarly recover information bitZ_{2k+1}. Finally, information bitZ_n will be demodulated according to the decision threshold.

$$b_n = \begin{cases} 1, & b_n > 0 \\ -1, & b_n \leq 0 \end{cases}. \tag{22}$$

where x_i satisfies the following conditions

$$x_{(2k+1)M+m} = x_{2(k+1)M+m}, 0 < m \leq M; k \in \mathbb{Z}. \tag{23}$$

4.3 Simulation results

In order to display the complex dynamic characteristics of the generated hyperchaotic sequence, we use three groups of chaotic models as the RM-DCSK scheme chaotic sequence generators. The chaos model of the first group is the classical Logistic map, Sine map, and Tent map. While the second group was the memristor model proposed in reference[27], We generated two-dimensional memristor models based on the classical Logistic map, Sine map, and Tent map, denoted as 2D-MLM, 2D-MSM, 2D-MTM, respectively. The last group is three two-dimensional memristor models constructed in this paper. We use the above three groups of chaotic sequence generators to simulate the RM-DCSK scheme. The bit error rates (BERs) is calculated under different signal-noise-rate (SNR) and spread spectrum factor M. Note that each experiment transmits data in a randomly generated binary sequence of 10^5 bits. The initial conditions and control parameters of these models are listed in Table 4, which can make these models in a state of chaos.

Firstly, the RM-DCSK scheme with different SNR are considered. By setting SNR$\in \{0, 1, 2, \cdots, 30\}$ and fixing M = 300, we simulated the RM-DCSK scheme using three groups of chaotic sequence,respectively. The BERs of the demodulated and modulated signal under different SNR is shown in Fig.9(a). It can be seen that when the spectrum factor M is determined, when SNR is small, the models based on three groups of chaotic sequence generators can obtain almost the same BERs. However, the model based on the third group of chaotic sequence can obtain a smaller BERs than the first two groups of chaotic sequence with the increase of SNR. Furthermore, By setting M$\in \{260, 260, 270, \cdots, 350\}$ and fixing SNR = 18, we also simulated the RM-DCSK scheme using three groups of chaotic sequence, respectively. The BERs of the demodulated and modulated signal under different spectrum factor M is depicted in Fig.9(b). As shown, the model based on the third group of chaotic sequence can obtain a smaller BERs than the first two groups of chaotic sequence under different M. Chaotic system is used in secure communication. The distribution of chaotic output sequence is a key factor affecting transmission efficiency. Therefore, compared with the first two groups of chaotic sequence generators, the third group of chaotic sequence generators is more suitable for chaotic secure communication.

5 Conclusion

As the fourth basic circuit component, the memristor is a nonlinear function. If the memristor is introduced

Table 4 The initial conditions and control parameters of these models

Iterms	initial conditions	control parameters
Logistic	$x_0 = 0.4$	$\mu = 3.87$
Sine	$x_0 = 0.2$	$\mu = 0.95$
Tent	$x_0 = 0.3$	$\mu = 1.47$
2D-MLM	$x_0 = 0.5,\ q_0 = 0.5$	$\mu = 0.1,\ k = 1.88$
2D-MSM	$x_0 = 0.4,\ q_0 = 0.7$	$\mu = -0.1,\ k = 1.78$
2D-MTM	$x_0 = 0.3,\ q_0 = 0.6$	$\mu = -0.3,\ k = 1.68$
2D-DMLM	$x_0 = 0.2,\ q_0 = 0.3$	$\mu = 0.2,\ k = 1.99$
2D-DMLM	$x_0 = 0.4,\ q_0 = 0.1$	$\mu = -0.05, k = 1.82$
2D-DMTM	$x_0 = 0.2,\ q_0 = 0.6$	$\mu = -0.4,\ k = 1.58$

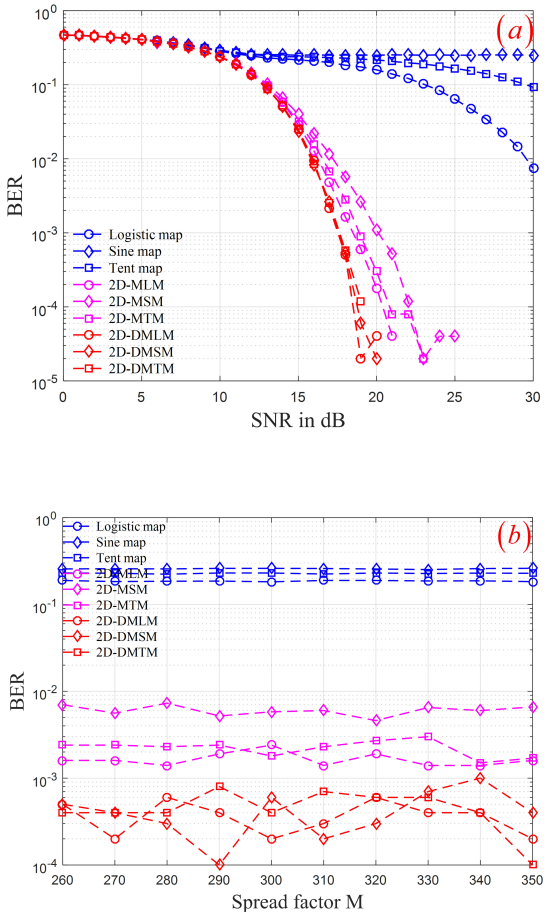

Fig. 9 BERs of the RM-DCSK using three groups of chaotic sequence:**a** different SNR, **b** different M

into the chaotic circuit, the complexity of the circuit can be strengthened. In this paper, we discretized the ideal flow-controlled memristor model by Eluer method, and then obtained the discrete memristor model, and coupled the discrete memristor model with the one-dimensional discrete chaotic system to obtain the two-dimensional discrete memristor coupling model. In chapter 3, three real numerical examples are given. Lyapunov index, bifurcation diagram and chaotic hyacinth are used to show that the dynamic behavior of the system has been significantly improved. Secondly, the system has high complexity through sample entropy, permutation entropy, correlation dimension and Kaplan-Yorke dimension. Finally, the model proposed in this paper is applied to secure communication. Compared with the one-dimensional chaotic system and the existing two-dimensional memristor model, the transmission efficiency of the model proposed in this paper is significantly improved. Therefore, by coupling the model with the discrete memristor, the dynamic characteristics of the low-dimensional chaotic system can be enhanced.

Acknowledgements This research was funded by the National Natural Science Foundation of China, and grant number is 61471158.

Data availability statement

Data sharing not applicable to this article as no datasets were generated or analysed during the current study.

Conflict of interest

The authors declare that they have no conflict of interest.

References

1. Chua L.O.: Memristor-the missing circuit element. IEEE Trans. Circuit Theory, **18**, 507-51 (1971)
2. Chua, L.O., Kang, S.M.: Memristive devices and systems. Proc IEEE **64**, 209-223 (1976)
3. Strukov, D.B., Snider, G.S., Stewart, D.R., Williams, R.S.: The missing memristor found. Nature **453**, 80-83 (2008)
4. Adhikari, S.P., Sah, M.P., Kim, H., Chua, L.O.: Three fingerprints of memristor. IEEE Trans. Circuits Syst. I Reg. Papers **60**, 3008-3021 (2013)
5. Sun, J., Yao, L., Zhang, X., Wang, Y., Cui, G.: Generalised mathematical model of memristor. Iet Circ. Device. Syst. **10**, 244-24 (2016)
6. Wang, C., Xiong, L., Sun, J., Yao, W.: Memristor-based neural networks with weight simultaneous perturbation training. Nonlinear Dyn. **95**, 2893–2906 (2018)
7. Duan, S., Hu, X.,Dong, Z., Wang, L., Mazumder, P.: Memristor-based cellular nonlinear/neural network: design, analysis, and applications. IEEE Trans. Neural. Netw. Learn. Syst. **26**, 1202-121 (2015)
8. Zhang, Y., Zhuang. J., Xia, Y., Bai, Y., Cao. J., Gu, L.: Fixed-time synchronization of the impulsive memristor-based neural networks. Commun.Nonlinear Sci. **77**, 40–5 (2019)
9. Yuan, F., Li, Y.: A chaotic circuit constructed by a memristor, a memcapacitor and a meminductor. Chaos **29**, 101101 (2019)

10. Fang, Y., Yue, D., Li, Y., Wang, G.: The amplitude, frequency and parameter space boosting in a memristor–meminductor-based circuit. Nonlinear Dyn. **96**, 389–40 (2019)
11. Ghenzi, N., Levy, P: Impact of sub- and supra-threshold switching in the synaptic behavior of TiO2 memristor. Microelectron. Eng. **193**, 13-17 (2018)
12. Wang, Y., Ma, J., Xu, Y., Wu, F., Zhou, P.: The electrical activity of neurons subject to electromagnetic induction and gaussian white noise. Int J Bifurc Chaos **27**, 175003 (2017)
13. Kim, H.,Sah, M.P., Yang, C., Cho, S., Chua, L.O.: Memristor emulator for memristor circuit applications. IEEE Trans. Circuits Syst. I Reg. Papers **59**, 2422-243 (2012)
14. Lorenz, E. N. : Deterministic nonperiodic flow. J. Atoms. **20**, 130-141 (1976)
15. Song, S.X., Liu, J.X., Yun. Q.L., Y.L., Cao. L.C., Harkin.: Counteracting dynamical degradation of digital chaotic chebyshev map via perturbation. Int J Bifurc Chaos **27**, 130-141 (2017)
16. Zheng, J., Hu, H.P., Xia, X. : Applications of symbolic dynamics in counteracting the dynamical degradation of digital chaos. Nonlinear Dyn. **94**, 1535-1546 (2018)
17. Zhou, Y., Bao. L., Chen. C.: Image encryption using a new parametric switching chaotic system.Signal Process. **93**, 3039–3052 (2013)
18. Hua, Z., Zhou, B., Zhou, Y.: Sine-transform-based chaotic system with FPGA implementation.IEEE Trans. Ind. Electron. **65**, 2557-2566 (2017)
19. Hua, Z., Zhou, Y., Huang, H.: Cosine-transform-based chaotic system for image encryption.Inf. Sci. **480**, 403-419 (2019)
20. Itoh, M., Chua, L. O.: Memrsitor Oscillator.Int J Bifurc Chaos **18**, 3183-3206 (2008)
21. Zhang, Y., Liu, Z., Wu, H., Chen, S., Bao, B.: Two-memristor-based chaotic system and its extreme multistability reconstitution via dimensionality reduction analysis.Chaos Solit. Fractals **127**, 354–363 (2017)
22. Ma, J., Wu, F.Q., Ren, G.D., Tang, J.: A class of initials-dependent dynamical system. Appl. Math. Comput. **298**, 65-76 (2017)
23. Zhou, L., Wang, C.H., Zhang,X., Yao, W.: Various attractors, coexisting attractors and antimonotonicity in a simple fourth-order memristive Twin-T oscillator. Int J Bifurc Chaos **28**, 1850050 (2018)
24. Lai, Q., Kuate, P., Liu, F., Iu, H.C.: An extremely simple chaotic system with infinitely many coexisting attractors. IEEE Trans. Circuits Syst. II: Exp. Briefs **67**, 1129-1133 (2019)
25. Varshney, V., Sabarathinam, S., Awadhesh, P., Thamilmaran, K.: Infinite number of hidden attractors in memristor-based autonomous duffing oscillator. Int J Bifurc Chaos **67**, 1129-1133 (2019)
26. Peng, Y., Sun, K., He, S.: A discrete memristor model and its application in Hénon map. Chaos, Solit. Fractals **137**, 109873 (2020)
27. Bao, B., Rong, K., Li, H., Li, K., Hua, Z., Zhang, X.: Memristor-coupled Logistic hyperchaotic map. IEEE Trans. Circuits Syst. II: Exp. Briefs **68**, 2992-2996 (2021)
28. Deng, Y., Li, Y.: Nonparametric bifurcation mechanism in 2-D hyperchaotic discrete memristor-based map. Nonlinear Dyn. **104**, 4601-4614 (2021)
29. Chua, L.O: If it's pinched it's a memristor. Semicond. Sci. Tech. **29**, 104001 (2014)
30. Richman,J., Moorman, J.: Physiological time-series analysis using approximate entropy and sample entropy. Am J Physiol. Heart Circ. Physiol. **278**, 2039-2049 (2000)
31. Bandt, C., Pompe, B.: Permutation entropy: a natural complexity measure for time series. Phys. Rev. Lett. **88**, 174102 (2002)
32. Theiler, J.: Efficient algorithm for estimating the correlation dimension from a set of discrete points. Phys. Rev. A. **36**, 4456-4462 (1987)
33. Frederickson, P., Kaplan, J., Yorke, E., Yorke, J.: The liapunov dimension of strange attractors. J. Differ. Equ. **49**, 185-207 (1983)